Strings of Liquid Beads for Gas-Liquid Contact Operations

Kenji Hattori, Mitsukuni Ishikawa, and Yasuhiko H. Mori
Dept. of Mechanical Engineering, Keio University, Yokohama 223, Japan

A novel device for gas-liquid contact operations is proposed to feed a liquid onto wires (or threads) hanging down in a gas stream is proposed. The liquid disintegrates into beads strung on each wire at regular intervals; if the wire is moderately wettable, a thin film forms to sheathe the wire, thereby interconnecting the beads. Since the beads fall down slowly, which possibly renews the film flowing down even more slowly, a sufficient gas-liquid contact time is available even in a contactor with considerably limited height. An approximate calculation method is developed for predicting the variation in the temperature effectiveness for the liquid (the fractional approach of the liquid exit temperature to the gas inlet temperature) with the falling distance, assuming an applicability of strings-of-beads contactors to thermal energy recovery from hot gas streams.

Introduction

Energy recovery from hot gases exhausted from power plants, garbage incineration facilities, and many industrial processes has been growing due to demands for saving the primary-energy consumption and, probably to a much lesser extent, for the protection of the environment. Further extension of such energy recovery depends on the development of efficient heat exchange devices which are low cost, easy to maintain, and in some applications adaptable to periodic or interminable changes in flow rates and/or temperature levels of the heat-source gas streams. For example, buoyancy-driven hot-air flows available in storage facilities of vitrified packages of radioactive wastes (Tani, 1989) must decay interminably over a prescribed storage period (typically several decades). Heat exchangers with rigid structures are hardly suited to such time-varying gas flows. The most promising selection for this sort of gas flows is direct-contact gas-liquid heat exchangers, in which the magnitude of hydrodynamic resistance exerted on the gas flows can readily be changed with alterations of some inserts such as spray nozzles, baffles, packings, and so on. In fact, this study was first motivated by an inquiry from the nuclear industry in Japan about the utility of spray columns for thermal-energy recovery from buoyant flows of air having been used to cool packages of radioactive wastes. The use of direct gas-liquid contactors of any type has another advantage in that the pollutants, if any, carried by the gases are removed to some extent by the liquids.

There are several different types of gas-liquid contact devices usable for the operation of gas-to-liquid (or liquid-to-gas) heat and/or mass transfer. Wetted-wall, spray, bubble-tray, and packed columns are among the conventional types. Fair (1990), for example, described methods for designing columns of some different types for the recovery of energy from hot gas discharge streams. The methods are based on the accumulated experience with gas-liquid contactors for mass-transfer applications such as absorption, desorption, humidification, and dehumidification (Treybal, 1955).

When the available gas flow has a rather low dynamic pressure, the first choice of the contactor type may be a spray column which provides a large gas-liquid interfacial area without exerting a great hydrodynamic resistance to the gas flow. However, the spray column is not necessarily suitable for the purpose of energy recovery from the gas by means of direct-contact sensible-heat transfer to a nonvolatile liquid. The large free-fall velocity of the liquid disintegrated into drops gives a large gas-to-liquid heat-transfer coefficient but results in a short gas-liquid contact time in the column and thus inevitably a rather low level of the *temperature effectiveness for the liquid* (the fractional approach of the liquid exit temperature to the gas inlet temperature). Since the level of the temperature effectiveness is generally more important than the rate of heat removal from the gas, some means to reduce the fall velocity

Correspondence concerning this article should be addressed to Y. H. Mori.
Current address of K. Hattori: NTT Chiba Network Center, Chiba 260, Japan.
Current address of M. Ishikawa: Nikko Gould Foil Co. Ltd., Hitachi 317, Japan.

and thereby extend the residence time of the liquid in the column of a given height is desirable. An analogous problem may be found in some mass-transfer processes. The liquid-side *mass-transfer efficiency*, the analog to the *temperature effectiveness*, can rarely be high enough in ordinary spray columns.

In this article we propose a novel device which will possibly be a solution to the problem stated above: to feed a liquid onto wires (or threads) hanging down in a gas stream. The liquid flows down on each wire taking the form of discrete drops sliding on the wire, or a thin liquid film coating the wire, thereby giving the appearance of a "string of beads" traveling down. The gas may flow up countercurrently with the "strings of liquid beads," or may flow horizontally, crossing a bundle or a curtain of the "strings." This device will provide a sufficient gas-liquid contact time, even if the liquid falling distance is substantially limited, while retaining the advantages of spray columns such as large gas-liquid interfacial area per unit volume and small pressure drop in the gas stream. In the following, we describe experimental observations of the dynamic behavior of liquid flow on wires and an approximate analysis for calculating the variations with the falling distance of the temperature effectiveness for heating (or cooling) the liquid.

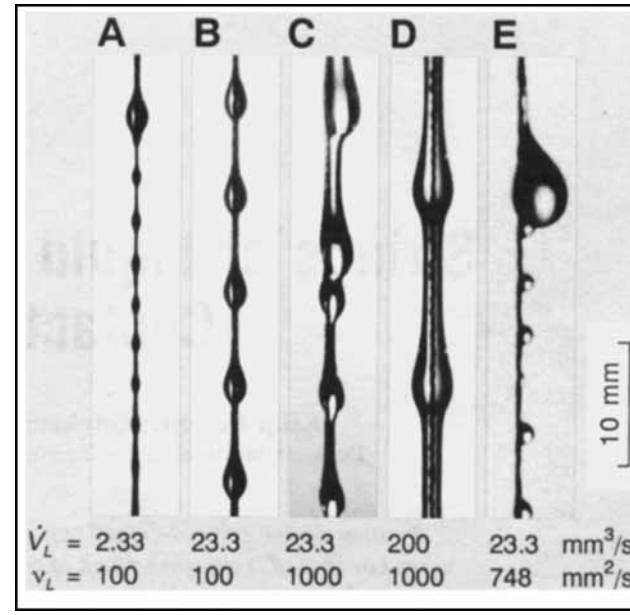

Figure 1. Typical flow patterns of silicone oils on a 0.4-mm-dia. Teflon thread (pictures A-D) and glycerol of a 0.5-mm-dia. Teflon-coated glass thread (picture E).

Experimental Observations

The mechanisms of liquid flow on wires or fibers has not been studied extensively. Recently, Quéré et al. (1990) and Quéré (1990) reported elegant studies on spreading and film/drop flow of liquids on fibers. Although these studies are very instrumental to the understanding of the capillarity of liquids on fibers, they do not provide solutions to the problems that we encounter in considering "strings-of-beads" contactors: they are how the flow pattern varies with the flow rate imposed on each wire, and how fast liquid drops and films flow down on the wire. With the objective of obtaining empirical solutions to these capillary-hydrodynamic problems, we have performed simple experiments under isothermal conditions.

Procedure and materials

A wire or a 1.5-m-long thread was hung vertically in laboratory air controlled at 26 ± 1°C. A liquid was supplied at a constant rate from a syringe-infusion pump onto the wire (or thread) at its top, and the behavior of the liquid while flowing down on the wire (or thread) was observed. Teflon threads (0.4 and 1.6 mm in diameter) and a Teflon-coated glass thread (0.5 mm in diameter) were prepared for use as sample threads having low surface free energies, while a stainless steel wire (0.3 mm in diameter) was employed as a sample having a high surface free energy. The liquids tested were dimethyl silicone oils (KF 96 series prepared by Shin-etsu Chemicals Co., Tokyo), water, and glycerol. The silicone oils have considerably different viscosities ($\nu_L = 10^2$–10^3 mm^2/s), while all of them have nearly the same, rather low surface tensions (~21 mN/m). Water and glycerol are greatly different in viscosity ($\nu_L = 0.89$ and 748 mm^2/s, respectively), but they are closely related with respect to their surface tensions (72.7 and 63.4 mN/m, respectively), which are a few times higher than those of the silicone oils.

It should be noted that the surfaces of the wire and the threads as well as the liquids were prepared under "practical conditions," that is, without rigorous cleaning or purification. The wire and the threads were washed in an ultrasonic cleaning bath filled with a detergent solution, then rinsed in the same bath while the detergent solution was continuously replaced with tap water, and finally rinsed with a large quantity of running distilled water. Although sufficient care was taken to prevent them from being contaminated with human skin oil during their washing, rinsing, or drying in a vacuum chamber and setting for the observations, they must have suffered atmospheric contamination. Thus, the stainless steel wire we used is not considered to have been a high-energy material in the strict sense (Schrader, 1974), although we call it that by comparison with Teflon and Teflon-coated glass threads. The silicone oils and the glycerol (reagent grade) were used as received from the suppliers. Water was purified by deionization and distillation.

Results of observations

Observations with the solid and the liquid samples mentioned above have revealed that the flow behavior of a liquid on a wire or a thread is primarily dependent on its diameter and liquid wettability and also on the flow rate of the liquid. Every silicone oil wets well every wire or thread and thus forms a thin annular film covering it. Except for the thickest thread, 1.6 mm in diameter, bead-like liquid drops slide down on the film intermittently. The flow behavior in this class may be divided into four patterns (A to D), as demonstrated in Figure 1, depending on the flow rate, $\dot{V}_L$, and the viscosity of the liquid. At sufficiently low flow rates, drops spontaneously formed near the top end of the wire or thread fall down at regular intervals. Each of these "primary" drops trails a film, which in turn breaks into tiny "secondary" drops due to the Rayleigh instability, still leaving a thin film connecting these drops. The secondary drops thus formed are then swallowed

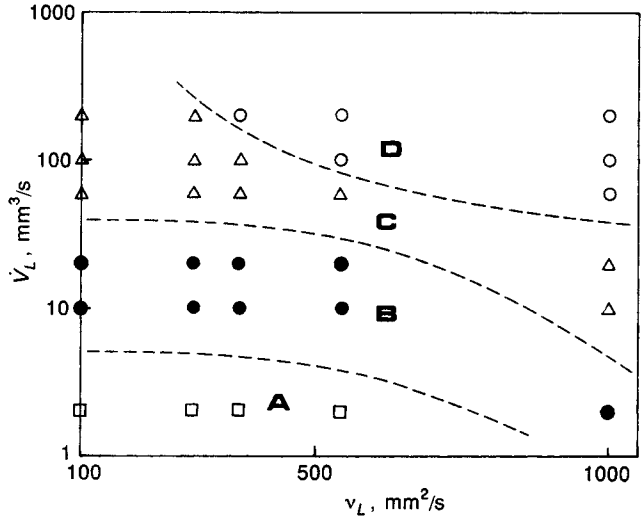

Figure 2. Map for flow patterns of silicone oils on a 0.4-mm-dia. Teflon thread.

by the succeeding primary drop. Due to a balance between engulfing the secondary drops and trailing a film, each primary drop almost maintains a constant size as it falls down over the entire length of the wire or thread. This pattern, which we refer to as pattern A, seems to be essentially the same as the one described by Quéré et al. (1990). As the flow rate is increased, the interval of the fall of the primary drops becomes too short to permit the film left behind each primary drop to break into secondary drops. Thus we observe monosize drops and monolength cylindrical sheaths of the liquid alternately aligned in the appearance of a "string of beads" (pattern B). With the flow rate and/or the viscosity of the liquid increasing further, the high regularity of the liquid motion observed in pattern B is lost. Drops of different sizes fall at different velocities, repeating mutual integrations and disintegrations (pattern C). At even higher flow rates and/or viscosity such a regularity as that characterizing pattern B is recovered again. Monosize drops fall at regular intervals, although an annular film much thicker than those observed in pattern B bridges over each interval (pattern D). The four patterns (A-D) observed with the silicone oils supplied onto the 0.4-mm-dia. Teflon string are mapped in Figure 2.

On the thicker 1.6-mm-dia. Teflon thread every silicone oil flows down forming an annular film, which is apparently uniform over the entire length of the thread. No drop formation is observed. This finding is presumably ascribable to a reduction with an increase in the thread diameter of the driving force for developing the Rayleigh instability of the film, which is no more than an axial capillary-pressure gradient to be generated in the film in response to some disturbances. A simple consideration of the instability kinetics described in Appendix A predicts a strong negative dependency of the capillary-pressure gradient on the thread diameter and thus supports the above interpretation of the apparent vanishment of bead-like drops on the thick thread.

Neither water nor glycerol wets any wire or thread so well as to form a regular beads-and-film pattern. On contact with the wire (or thread), these liquids immediately disintegrate into discrete drops, which helically roll down on the wire (pattern

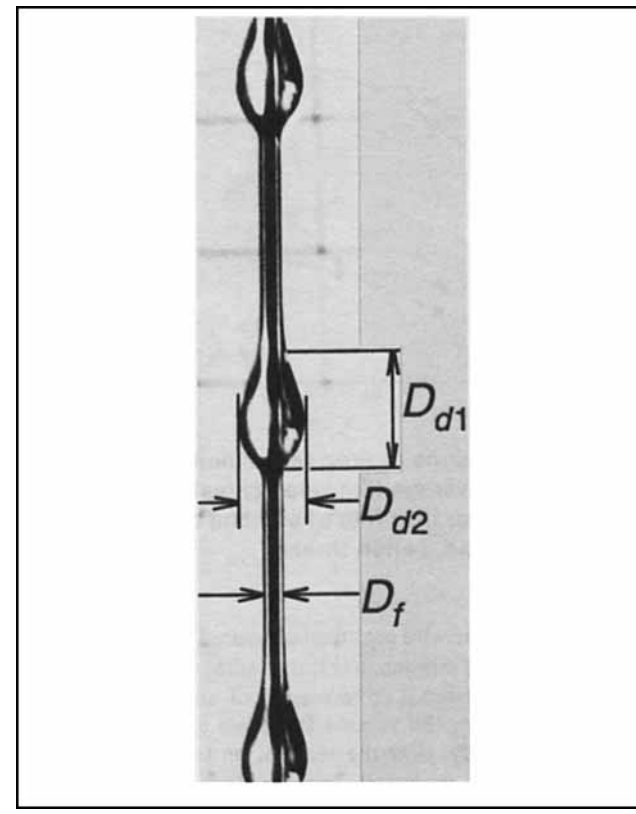

Figure 3. Characteristic dimensions of a drop and a cylindrical film-coated portion.

It shows a flow of silicone oil, $\nu_L = 100$ mm²/s, on a 0.3-mm-dia. stainless-steel wire.

E). Water drops thus rolling down leave the wire surface behind them dry. Glycerol which is much more viscous than water shows a slightly different behavior: each of the "primary" drops rolling down trails a liquid film or string, which disintegrates into "secondary" drops sticking to the wire surface. These secondary drops are engulfed by the succeeding primary drop. The distinguishing features of this flow pattern such as the wetting of only a quite small portion of the wire surface and the comparatively large size of the primary drops are ascribable to the two physicochemical properties of the solid-liquid pairs in question: the poor wettability of the wire surface with the liquids and the large surface tensions of the liquids themselves. The effects of these two properties are more or less interrelated, and no clear-cut evaluation of each effect can be provided at present.

In the regime of pattern B we have measured the fall velocities, U_d, and time intervals, τ, of drops by naked-eye observations with the aid of a stopwatch. At the same time, we have measured the dimensions of drops and films by projecting their horizontally-viewed images on a Nac 35-mm film analyzing system at a large magnification, as indicated in Figure 3. They are D_{d1}, the longitudinal distance between the maximum curvature points on the horizontally-viewed liquid surface that bound each drop; D_{d2}, the maximum horizontal dimension of each drop; and D_f, the diameter of each cylindrical portion interposing two neighboring drops. The drop dimensions thus measured have been used to calculate D_d, the effective diameter, as $D_d = (D_{d1}D_{d2}^2)^{1/3}$. The data of D_f and D_s,

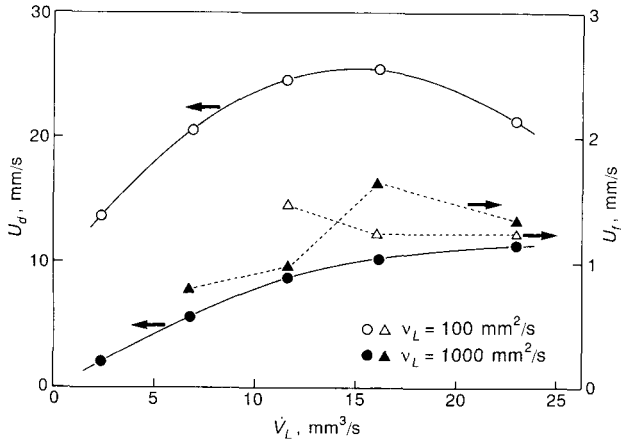

Figure 4. Variations in drop fall velocity (observed), U_d, and average film velocity (estimated), U_f, with volume flow rate of silicone oil fed onto a 0.4-mm-dia. Teflon thread.

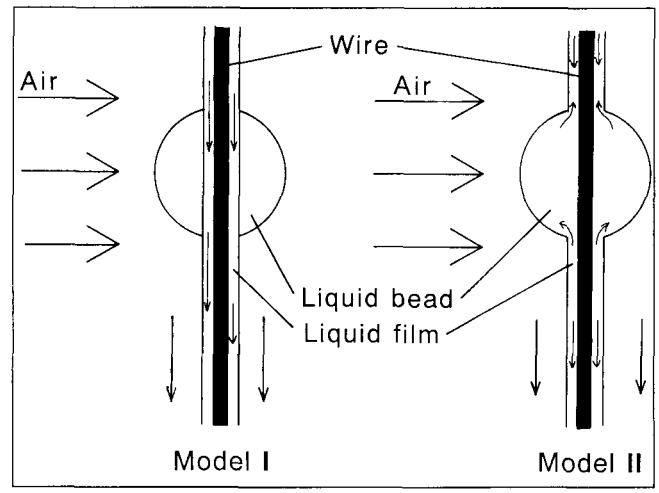

Figure 5. Analytic models for heat transfer to liquid flowing down on a vertical wire.

the diameter of the wire or thread measured with a micrometer, have been used to estimate $u(r)$, the radial distribution of flow velocity in a horizontal cross section of an annular film, and then $\dot{V}_{L,f}$ and U_f, the volume flow rate and the average velocity, respectively, over the section, on the assumption of a developed axially-symmetric laminar flow on a smooth cylindrical surface of diameter D_s. Appendix B is devoted to discussing the validity of the developed-flow assumption, as well as to deriving mathematical expressions for $u(r)$, $\dot{V}_{L,f}$ and U_f based on the assumption.

The variations in U_d and U_f with $\dot{V}_L$, the volumetric rate of liquid supply onto each wire or thread, are exemplified in Figure 4. It should be noted that each data point for U_d represents the mean of the data obtained with different drops falling successively under the same operational condition. The scatter of the data about the mean is within a few percent. The uncertainty for each point for U_f is mostly associated with the measurement of D_f and is estimated to be $-9/+16\%$ at the most. Here we find that the magnitude of U_d is larger than that of U_f typically by one order. It may be interesting to note that U_d peaks at an intermediate level of $\dot{V}_L$ when ν_L is not too high. The variations in D_d with $\dot{V}_L$ are not significant throughout the regime of pattern B. On the 0.4-mm-dia. Teflon thread, for example, D_d observed with a less viscous silicone oil ($\nu_L = 100$ mm^2/s) is 2.0 ± 0.2 mm, while D_d observed with a more viscous oil ($\nu_L = 1{,}000$ mm^2/s) gradually increases from ~ 2.0 to ~ 2.8 mm as $\dot{V}_L$ increases.

We have observed no sign that the nature of liquid flow as stated above may depend more than slightly on the material or the surface roughness of the wire or thread so far as it is well wetted by the liquid. It may be worth noting that $\dot{V}_{L,f}$, the liquid flow rate predicted on the assumption of simple annular film flow with outside diameter D_f (Appendix B), is no more than several percent of $\dot{V}_L$. Evidently, it is not films but drops that play the major role in conveying the liquid along the wire or thread.

In practical applications such as those discussed in the introduction section, the liquid flowing on wires or threads will necessarily be subjected to a steady gas stream. If the stream is crossing the wires or threads and is so strong that its dynamic head approaches, or even exceeds, the capillary pressures due to the curvatures at the surfaces of the drops and films, their configurations may be appreciably distorted. When the gas stream is a countercurrent with the liquid flow, the fall of drops will be more or less retarded. These effects are estimated to be insignificant when, for example, drops a few millimeters (or less) in D_d are exposed to a low pressure (~ 0.1 MPa) gas stream up to several meters per second in undisturbed velocity. Considering the approximate nature of the analysis of heat transfer to the liquid from a gas stream, which is described in the next section, we will use the above results of liquid flow observations under no gas flow to supplement the analysis to predict the temperature change in the liquid with the fall distance in the subsequent section.

Analysis of Heat Transfer

A liquid flow of pattern B is on an isolated wire (or thread) exposed to a uniform cross flow of a hot gas. The liquid is assumed to be nonvolatile, and hence a simple sensible-heat-transfer process accompanied with no mass transfer is dealt with here. Two extreme models, as illustrated in Figure 5, are conceived for ease of analysis. Model I assumes that the drops simply slide down on an annular film, causing no mass and energy exchange between the drops and the film. Model II assumes that each drop engulfs an annular film ahead of itself and so rebuilds the film that it is drawn out from the rear of the drop, having an initial temperature equal to the mixed mean drop temperature at each instant. The additional assumptions common to both models are:

(1) The film and the drop form a uniform cylinder and a sphere, respectively, both coaxial with the wire.

(2) The sizes and the velocities of the film and the drop are held constant while falling on the wire.

(3) The axial heat conduction inside the wire is neglected.

(4) The average coefficient for gas-to-drop surface heat transfer is approximated by Ranz and Marshall's correlation (Ranz and Marshall, 1952) for an isolated sphere of diameter D_d held stationary in a gas stream, on the condition that the oncoming gas velocity, U_G, is much higher than the drop velocity, U_d, and that the effective heat-transfer area is evaluated to be $\pi(D_d^2 - D_f^2/2)$.

(5) The average coefficient for gas-to-film surface heat transfer, α_f, is given by Churchill and Bernstein's correlation (Churchill and Bernstein, 1977) for a cross flow over a cylinder.

(6) The coefficient for heat transfer inside the drop is provided by either of the two limiting asymptotic solutions for transient heat transfer inside a sphere: the Newman solution for purely conductive heat transfer and the Kronig-Brink solution assuming a toroidal circulation fully developed inside a sphere (Clift et al., 1978a).

(7) The gas-to-drop overall heat-transfer coefficient, α_d, is simply evaluated as the reciprocal of the sum of the reciprocals of the gas-side and the liquid-side heat-transfer coefficients evaluated independently as stated above.

(8) The film shows a negligibly small resistance against the radial gas-to-film heat transfer.

(9) The axial heat conduction through the film can be neglected.

(10) The physical properties of the gas and the liquid are constant.

Assumption 6 may need some explanation. The drops of the present interest undergo shear stress on the surface of the wire piercing them. The stress may cause such a toroidal circulation in each drop that it resembles that developed inside a drop falling in a medium of relatively high viscosity, thereby suffering tangential stress on its surface. (The direction of the former circulation relative to the gravity vector must be opposite to that of the latter, but this difference is of no concern to the present problem.) Thus, it seems reasonable to assume that the Kronig-Brink solution for freely falling (or rising) drops with internal circulation (Clift et al., 1978a) approximates the heat transfer inside drops falling on the wire. The Newman solution for drops with no internal motion presumably gives the possible minimum of the internal heat-transfer coefficient. The Kronig-Brink solution is incorporated into both model I and model II. On the other hand, the Newman solution is incorporated only into model I, because it is evidently inconsistent with model II which necessarily assumes convective liquid mixing inside the drops.

Assumption 8 may appear to be disputable. Its validity is examined by an approximate analysis of heat transfer into the film, which is described in Appendix C.

Formulation for model I

The energy conservations for each drop and a unit-length element of the film are written, respectively, as follows:

$$\rho_L c_L V_d \frac{dT_d}{dt} = A_d \alpha_d (T_G - T_d) \tag{1}$$

$$\rho_L c_L S_f \frac{dT_f}{dt} = \pi D_f \alpha_f (T_G - T_f) \tag{2}$$

where

$$V_d = \pi\left(\frac{D_d^3}{6} - \frac{D_d D_f^2}{4}\right)$$

$$A_d = \pi\left(D_d^2 - \frac{D_f^2}{2}\right)$$

$$S_f = \frac{\pi}{4}(D_f^2 - D_s^2)$$

The initial condition common to both T_d and T_f is given by simply defining the initial liquid temperature, T_{L0}, as:

$$t=0: \quad x=0, \quad T_d = T_f = T_{L0} \tag{3}$$

Integrating Eqs. 1 and 2 under the initial condition given above, we get:

$$\frac{T_d - T_{L0}}{T_G - T_{L0}} = 1 - \exp\left(-\frac{A_d \alpha_d t}{\rho_L c_L V_d}\right) \tag{4}$$

$$\frac{T_f - T_{L0}}{T_G - T_{L0}} = 1 - \exp\left(-\frac{\pi D_f \alpha_f t_{fg}}{\rho_L c_L S_f}\right) \tag{5}$$

The time lapse t in Eq. 4 and t_{fg} in Eq. 5, the sum of the periods in which the film element is exposed to the gas stream, can be related to x, the vertical distance traveled by the drop and the film element, as:

$$t = x/U_d \tag{6}$$

$$t_{fg} = \frac{x}{U_f}\left(1 - \frac{D_d}{\tau U_d}\right) \tag{7}$$

Substituting Eqs. 6 and 7 into Eqs. 4 and 5, respectively, we can evaluate $T_d(x)$ and $T_f(x)$. Once $T_d(x)$ and $T_f(x)$ are known, we can immediately calculate $T_L(x)$, the mixed mean temperature of the liquid as a function of the drop fall distance, as:

$$T_L(x) = \frac{T_d(x) V_d/\tau + T_f(x) S_f U_f}{V_d/\tau + S_f U_f} \tag{8}$$

Formulation for model II

The energy conservation for each drop is written as:

$$\rho_L c_L V_d' \frac{dT_d}{dt} = A_d \alpha_d (T_G - T_d) + \rho_L c_L S_f (U_d - U_f)(T_f - T_d) \tag{9}$$

where V_d' is the drop volume defined as:

$$V_d' = \pi\left(\frac{D_d^3}{6} - \frac{D_d D_s^2}{4}\right)$$

and T_f is the temperature of the film that the drop front just meets. Equation 9 is solved for T_d by an iterative procedure described below.

First we assume $T_f(x)$ arbitrarily, which is designated as $T_{f1}(x)$. Then we calculate, by numerically integrating Eq. 9, the temperature $T_{d1}(x)$ that a drop will have while falling down on the wire and thereby interacting with the film with temperature $T_{f1}(x)$. (Here x denotes the vertical position of the drop front at each instant.) The film rebuilt at the rear end of the drop is exposed to the gas stream for a period τ_{fg} and then meets the front of a second drop (see Figure 6). The temper-

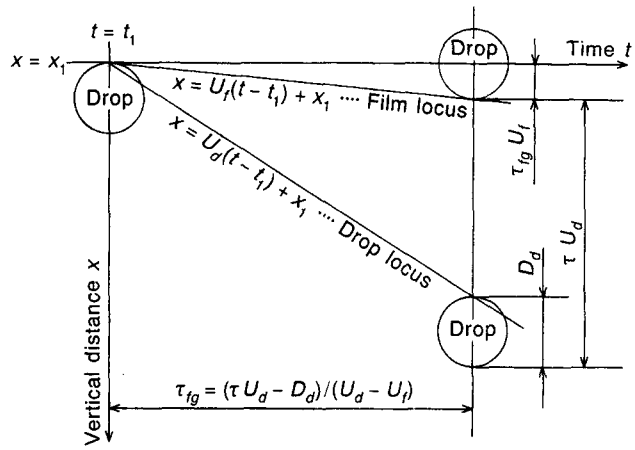

Figure 6. Estimating τ_{fg}, the period in which a film element is exposed to the gas stream.

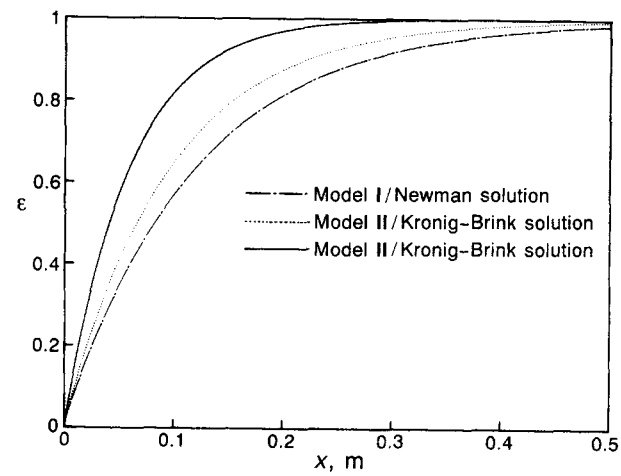

Figure 7. Heat-transfer efficiency vs. liquid fall distance: comparison of analytic models.

Silicone oil ($\nu_L = 100$ mm^2/s) fed onto 0.4-mm-dia. Teflon thread at $\dot{V}_L = 23.3$ mm^3/s in air stream, $U_G = 5.0$ m/s. The properties of the oil and air are evaluated at 101.3 kPa and 25°C, the conditions set in the experimental observations.

ature of the film at this instant, $T_{f2}(x)$, is obtained by integrating Eq. 2 over the period τ_{fg} as:

$$\frac{T_{f2}(x) - T_{d1}(x + D_d - U_f\tau_{fg})}{T_G - T_{d1}(x + D_d - U_f\tau_{fg})} = 1 - \exp\left(-\frac{\pi D_f \alpha_f \tau_{fg}}{\rho_L c_L S_f}\right) \quad (10)$$

where

$$\tau_{fg} = \frac{U_d\tau - D_d}{U_d - U_f}$$

The temperature $T_{d2}(x)$ that the second drop will have is obtained by substituting Eq. 10 into Eq. 9 and integrating it numerically. Analogous calculations for succeeding drops are needed till $T_{fi}(x)$ and $T_{di}(x)$ $[i = 1, 2, 3, \cdots]$ no longer change from drop to drop. The asymptotic values of $T_{fi}(x)$ and $T_{di}(x)$ thus determined are considered to represent the solution of Eq. 9—$T_f(x)$ and $T_d(x)$. Substituting them into Eq. 8, we can calculate $T_L(x)$.

Predictions of Liquid Temperature Change

Substituting observed values of D_d, D_f, τ, and U_d and also estimated values of U_f into the analytical results given in the preceding section, we can predict the change, with the fall distance x, in the liquid temperature, or the *temperature effectiveness* (Kays and London, 1964) defined as:

$$\epsilon = \frac{T_L - T_{L0}}{T_G - T_{L0}}$$

Figure 7 compares predictions based on different models and/or different solutions for "in-drop" heat transfer. As expected, model I incorporating the Newman solution gives the most conservative prediction of ϵ. Though complete confidence cannot be put in any prediction given there, we still assume that the one based on model II incorporating the Kronig-Brink solution is the most accurate for the reason described below.

It is well-known that when liquid drops are falling (or rising) freely, undergoing no interaction with any immobile objects such as wires, threads, or plane walls, even a trace amount of surfactant contaminant adsorbed at the surface of the drops can substantially subdue the circulations inside them (Clift et al., 1978b) and thereby deteriorate the internal heat transfer compared with the prediction due to the Kronig-Brink solution. On the other hand, a drop falling on a wire (or thread) inevitably experiences a shear force on the wire surface confined in the drop itself, which is opposite in direction to the gravitational force acting on the toroidal liquid mass in the drop. The moment caused by the above mentioned couple of forces should work as the dominant drop-rolling mechanism, which is essentially independent of the drop-surface contamination or a resultant spatial interfacial-tension variation. Therefore, we can safely assume that the drops of our interest involve some toroidal circulations which necessarily interact with the film coating the substrate wire. The above idea is partially supported by an experimental observation that a tracer dye added to the film surface at a particular location was mixed to some extent into drops when they passed by the location one by one.

Figure 8 compares predictions of ϵ in "on-wire" flows based on model II incorporating the Kronig-Brink solution with those for free fall of drops of the same size as that observed in the on-wire flows. In calculating ϵ in the free-fall case, we have substituted the magnitude of the vector sum of the gas velocity, U_G, and the instantaneous drop fall velocity, $U_d = gt = \sqrt{2gx}$, into the Ranz-Marshall correlation to evaluate the external heat-transfer coefficient and have either applied the Kronig-Brink solution to evaluate the internal heat-transfer coefficient or assumed complete mixing (that is, uniform temperature) inside drops. (It should be noted that the mixing inside the drops during free fall can be enhanced by prolate-oblate oscillations (Yao and Schrock, 1976) and hence the internal heat-transfer coefficient may exceed that given by the Kronig-Brink solution (Hijikata et al., 1985). This is the reason why we have used the complete-mixing assumption besides the Kronig-Brink solution.) Here we find that the liquid fall distance required for achieving a prescribed level of ϵ can be greatly reduced by replacing a free-fall operation with an on-wire flow operation.

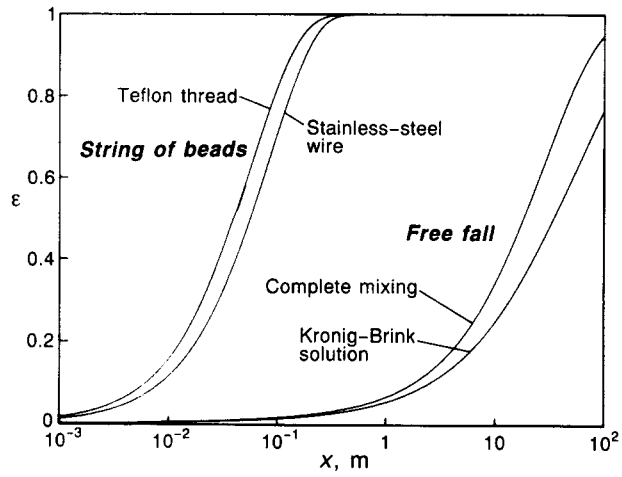

Figure 8. Heat-transfer efficiency vs. liquid fall distance: on-wire flow vs. free fall of silicone oil ($\nu_L = 100$ mm²/s) in air stream, $U_G = 5.0$ m/s.

For on-wire flow, $\dot{V}_L = 23.3$ mm³/s on 0.4-mm-dia. Teflon thread or 0.3-mm-dia. stainless-steel wire, and model II incorporating the Kronig-Brink solution is employed. For free fall, drop diameter is assumed to be 2.12 mm in agreement with D_d observed in the flow on the 0.4-mm-dia. Teflon thread.

Discussion

It has been demonstrated that "strings-of-beads flow" of a liquid on vertical wires or threads is an efficient means for achieving high liquid-side temperature effectiveness within a limited height permitted for the liquid to fall down, making contact with an ambient gas. The temperature effectiveness achieved at a given height may be controlled by selecting the liquids, since drop fall velocity, U_d, is significantly dependent on the viscosity of the liquid supplied onto the wires or threads (see Figure 4). Analogous claims may be made for mass transfer and simultaneous heat- and mass-transfer processes. The drawback of the on-wire operations lies in a limited flow-rate capacity for each wire or thread. The experimental observations summarized in Figure 2 suggest that the maximum flow rate in the regular strings-of-beads regime (pattern B), for example, will increase little even if we select liquids less viscous than those we have actually tested in this work. This drawback can be overcome, if necessary, by simply increasing the number density of wires or threads arranged in each gas-liquid contactor.

The analytic heat-transfer models presented in this article are rather crude. They are no more than tentative means to estimate, even though roughly, the performance of the on-wire flow device in heat- and/or mass-exchange operations. Detailed experimental observations are necessary to obtain not only full knowledge of apparent drop/film motions but also a good understanding of the flow structures in drop/film composites and thereby to prepare a more realistic model. An experimental study is also needed that actually investigates the gas-to-liquid (or liquid-to-gas) heat (and/or mass) transfer and tests the validity of the analytic models.

Notation

a = R_f/R_s
A_d = drop surface area
c = specific heat capacity
D_d = effective diameter of beadlike drop on wire evaluated as $(D_{d1}D_{d2}^2)^{1/3}$
D_{d1}, D_{d2} = major and minor axes of beadlike drop on wire
D_f = outside diameter of annular liquid film on wire
D_s = wire diameter
g = acceleration due to gravity
p = pressure
r = radial coordinate
r_f = local outside radius of disturbed annular liquid film on wire
R_f = outside radius of undisturbed annular liquid film on wire
R_s = wire radius
S_f = cross-sectional area of film
t = time or time lapse after the onset of liquid-gas contact
t_{fg} = sum of periods in which a film element is exposed to gas stream
T = temperature
T_b = mixed mean temperature in a cross section of liquid film
T_f = liquid-film temperature assumed to be radially uniform or film surface temperature (in Appendix C)
T_G = undisturbed gas temperature
T_L = mixed mean temperature of liquid
u = local velocity in liquid film
U_d = fall velocity of drop
U_f = average flow velocity in liquid film
U_G = undisturbed gas velocity
V_d = drop volume
$\dot{V}_L$ = volume flow rate of liquid
x = vertical distance traveled by liquid, being in contact with gas

Greek letters

α = gas-side or overall heat-transfer coefficient
δ = thickness of hydrodynamic boundary layer
ϵ = temperature effectiveness defined as $(T_L - T_{L0})/(T_G - T_{L0})$ or, only in Appendix A, amplitude of undulation of liquid film surface
η = dynamic viscosity
λ = wavelength of disturbance growing on liquid film surface or, when accompanied with a subscript G or L, thermal conductivity
ν = kinematic viscosity
ρ = mass density
$\Delta\rho$ = $\rho_L - \rho_G$
σ = surface tension of liquid
τ = time interval between successive drop falls on wire
τ_{fg} = period in which a film element is exposed to gas stream

Subscripts

d = drop
f = film
G = gas
L = liquid
max = maximum
min = minimum
0 = initial condition before the onset of liquid-gas contact

Literature Cited

Clift, R., J. R. Grace, and M. E. Weber, *Bubbles, Drops and Particles*, Academic Press, New York, p. 57 (1978a).
Clift, R., J. R. Grace, and M. E. Weber, *Bubbles, Drops and Particles*, Academic Press, New York, p. 38 (1978b).
Churchill, S. W., and M. Bernstein, "A Correlating Equation for Forced Convection from Gases and Liquids to a Circular Cylinder in a Crossflow," *Trans. ASME, J. Heat Transf.*, **99**, 300 (1977).
Fair, J. R., "Direct Contact Gas-Liquid Heat Exchange for Energy Recovery," *Trans. ASME, J. Solar Energy Eng.*, **112**, 216 (1990).
Hijikata, K., Y. Mori, and S. Kawaguchi, "Direct Contact Condensation of Saturated Vapor on a Falling Cooled Droplet (in Japanese)," *Trans. Jpn. Soc. Mech. Eng.*, **51B**, 152 (1985).

Kays, W. M., and A. L. London, *Compact Heat Exchangers*, 2nd ed., McGraw-Hill, New York, p. 15 (1964).
Ranz, W. E., and W. R. Marshall, Jr., "Evaporation from Drops, Part II," *Chem. Eng. Prog.*, **48**, 173 (1952).
Rayleigh, Lord, "On the Instability of a Cylinder of Viscous Liquid under Capillary Force," *Phil. Mag.*, **34**, 145 (1892).
Schlichting, H., *Boundary-Layer Theory*, 7th ed., McGraw-Hill, New York, pp. 90–91 (1979).
Schrader, M. E., "Wettability of Clean Metal Surfaces as Determined with Ultrahigh-Vacuum Techniques," *Fluid-Solid Surface Interactions, Proc. 2nd Symp.*, H. J. Lugt, ed., U.S. Naval Ship Res. Dev. Cent., Bethesda, Maryland, p. 151 (1974).
Tani, Y., "Development of Storage Technique for Vitrified Packages (in Japanese)," *Ishikawajima-Harima Eng. Rev.*, **29**, 322 (1989).
Treybal, R. E., *Mass-Transfer Operations*, McGraw-Hill, New York (1955).
Quéré, D., J.-M. di Meglio, and F. Brochard-Wyart, "Spreading of Liquids on Highly Curved Surfaces," *Sci.*, **249**, 1256 (1990).
Quéré, D., "Thin Films Flowing on Vertical Fibers," *Europhys. Let.*, **13**, 721 (1990).
Yao, S.-C., and V. E. Schrock, "Heat and Mass Transfer from Freely Falling Drops," *Trans. ASME., J. Heat Transf.*, **98**, 120 (1976).

Appendix A: Effect of Wire Thickness on the Rayleigh Instability

Here we assume a wire (or a thread) initially coated with an axisymmetric, axially uniform film of a liquid. When the film is subjected to infinitesimal disturbances, an axisymmetric undulation may be established on the surface of the film (Figure A1). In the following, we will estimate the magnitude of the axial capillary-pressure gradient, which is caused by the undulation and presumed to contribute to its further growth, that is, the establishment of the Rayleigh instability. Our particular interest is in finding out how the magnitude of the capillary-pressure gradient depends on the thickness of the wire.

Lord Rayleigh (1892) showed that the wavelength actually observed on the surface of a liquid cylinder corresponds to the fastest growing disturbance and is given by:

$$\lambda = 2\sqrt{2}\pi R_f \tag{A1}$$

where R_f denotes the radius of the cylinder in the absence of any disturbance. This expression for λ is also applicable to the instability of the annular film over the wire of a uniform radius R_s if ϵ, the amplitude of the surface undulation, is much smaller than the film thickness, $R_f - R_s$. The capillary pressure, that is, the pressure difference across the film surface, is practically given by σ/r_f, where σ is the surface tension of the liquid and r_f is the instantaneous local radius of the film surface. This is because the longitudinal curvature of the film surface must be much smaller than r_f^{-1}. The order of magnitude of $d(\sigma/r_f)/dx$, the axial gradient of the capillary pressure, is estimated with the aid of Eq. A1 as:

$$\frac{(\sigma/r_{f,\min}) - (\sigma/r_{f,\max})}{\lambda/2} \approx \frac{\sigma}{\lambda/2}\left(\frac{1}{R_f - \epsilon} - \frac{1}{R_f + \epsilon}\right) = \frac{\sigma}{\sqrt{2}\pi R_f}\left(\frac{2\epsilon}{R_f^2 - \epsilon^2}\right) \approx \frac{\sqrt{2}\epsilon}{\pi R_f^3} \tag{A2}$$

Since $R_f \sim R_s$, it turns out that the magnitude of the axial capillary-pressure gradient is approximately in inverse proportion to the cube of R_s or of the wire diameter D_s.

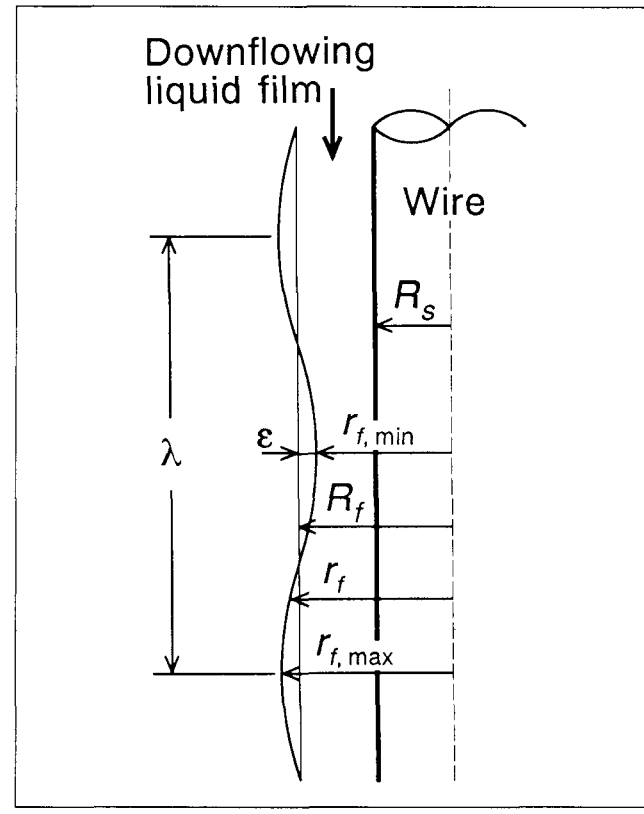

Figure A1. Disturbance growing on cylindrical liquid-film surface.

Appendix B: Annular Film Flow on a Vertical Wire

The annular liquid film on a wire is periodically disturbed by falling drops. The length of the period required for the film once disturbed to recover the steady-state flow profile within itself is considered first. For the purpose of order-of-magnitude estimation of the period, the film flow of the present interest may be replaced by a nonsteady parallel flow of a liquid adjacent to a flat plate which is suddenly set in motion in its own plane. This is generally referred to as Stokes' first problem (Schlichting, 1979). The solution of the latter problem gives $\delta(t)$, the instantaneous thickness of the boundary layer developing on the plate with t, the time lapse after the plate is set in motion, as:

$$\delta \approx 4\sqrt{\nu_L t} \tag{B1}$$

where ν_L is the kinematic viscosity of the liquid. The time required for δ to increase up to the dimension identical with the thickness of the annular film (0.1–0.25 mm when $\nu_L = 100$ mm^2/s; 0.3–0.4 mm when $\nu_L = 1{,}000$ mm^2/s) is calculated by use of the above solution as 0.5–45 μs, which is sufficiently short compared to τ, the interval of drop passage (0.1–0.4 s).

The above estimation of the flow-developing period for the annular film flow indicates that we can safely assume the flow to be always in a steady state to evaluate $u(r)$, $\dot{V}_{L,f}$ and U_f. Based on this idea, we then suppose a steady, axisymmetric, axially uniform, creeping flow of a liquid on a cylindrical, vertically oriented wire in a quiescent gaseous medium (Figure

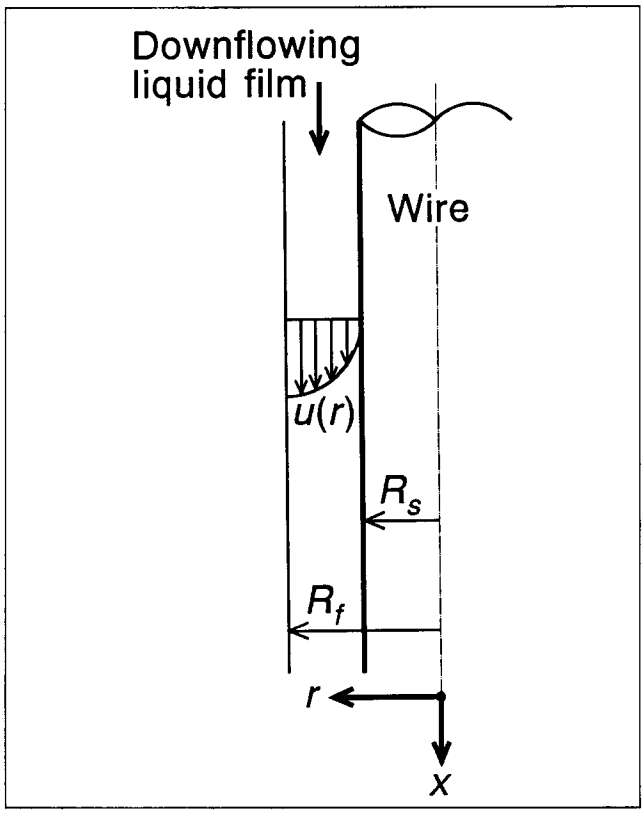

Figure B1. Annular liquid film downflowing on a vertical wire.

B1). The equations of motion for the flow may be written under the assumption of constant liquid properties as:

$$\eta_L \frac{1}{r}\frac{d}{dr}\left(r\frac{du}{dr}\right) = \frac{dp_L}{dx} - \rho_L g \tag{B2}$$

$$\frac{dp_L}{dx} = \frac{dp_G}{dx} = \rho_G g \tag{B3}$$

These equations are combined to give:

$$\frac{d^2u}{dr^2} + \frac{1}{r}\frac{du}{dr} = -\frac{\Delta\rho g}{\eta_L} \tag{B4}$$

Assuming zero shear stress at the gas-liquid interface, we write the boundary conditions as:

$$r = R_s: \quad u = 0 \tag{B5a}$$

$$r = R_f: \quad du/dr = 0 \tag{B5b}$$

The standard solution procedure of the above boundary-value problem gives:

$$u = \frac{\Delta\rho g R_s^2}{4\eta_L}(1 - \bar{r}^2 + 2a^2 \ln \bar{r}) \tag{B6}$$

where $\bar{r} \equiv r/R_s$ and $a \equiv R_f/R_s$. This solution can be used to calculate the volume flow rate, $\dot{V}_{L,f}$, and the average velocity, U_f, as:

$$\dot{V}_{L,f} = 2\pi \int_{R_s}^{R_f} rudr = 2\pi R_s^2 \int_1^a \bar{r}ud\bar{r}$$

$$= \frac{\pi\Delta\rho g R_s^4}{8\eta_L}(4a^2 - 3a^4 - 1 + 4a^4 \ln a) \tag{B7}$$

$$U_f = \frac{\dot{V}_L}{\pi(R_f^2 - R_s^2)} = \frac{\dot{V}_L}{\pi R_s^2(a^2 - 1)}$$

$$= \frac{\Delta\rho g R_s^2}{8\eta_L}\left(1 - 3a^2 + 4\frac{a^4 \ln a}{a^2 - 1}\right) \tag{B8}$$

Appendix C: Heat Transfer in Annular Film Flow on a Vertical Wire

Here we consider the heat transfer from the surface to the bulk of such an annular film as the one dealt with in Appendix B. The surface of the substrate wire is assumed to be adiabatic. The flow in the film is thermally developed, and the radial temperature distribution in the film is approximated by a quadratic function such that:

$$\frac{T - T_s}{T_f - T_s} = \left(\frac{r - R_s}{R_f - R_s}\right)^2 \tag{C1}$$

which satisfies the boundary condition:

$$r = R_s: \quad \partial T/\partial r = 0 \tag{C2}$$

The heat flux q_f at the film surface, $r = R_f$, is given by differentiating Eq. C1 as:

$$q_f = \lambda_L\left(\frac{\partial T}{\partial r}\right)_{r=R_f} = \frac{2\lambda_L}{R_f - R_s}(T_f - T_s) \tag{C3}$$

If we define the heat-transfer coefficient in the film, α_f, as:

$$q_f = \alpha_f(T_f - T_b) \tag{C4}$$

we have:

$$\alpha_f = \frac{2\lambda_L}{R_f - R_s}\frac{T_f - T_s}{T_f - T_b} \tag{C5}$$

where T_b is the bulk temperature in the film defined as:

$$T_b = \frac{1}{\dot{V}_L \rho_L c_L}\int_{R_s}^{R_f} 2\pi r \rho_L c_L u T dr \tag{C6}$$

The following is the calculation to rewrite T_b in terms of geometric parameters—R_f and R_s—in addition to T_f and T_s.

Substitution of Eq. C1 into Eq. C6 gives:

$$T_b = T_s + \frac{2\pi(T_f - T_s)}{\dot{V}_L (R_f - R_s)^2} \int_{R_s}^{R_f} ur(r - R_s)^2 dr$$

$$= T_s + \frac{2\pi(T_f - T_s) R_s^4}{\dot{V}_L (R_f - R_s)^2} \int_1^a u\bar{r}(\bar{r} - 1)^2 d\bar{r} \quad \text{(C7)}$$

Substituting Eq. B6 into the integrant in Eq. C7 and performing the integration, we get:

$$T_b = T_s + \frac{R_s^2 G(a)}{(R_f - R_s)^2} (T_f - T_s) \quad \text{(C8)}$$

where $G(a)$ is a function of a ($\equiv R_f/R_s$) such that:

$$G(a) = \frac{4}{4a^2 - 3a^4 - 1 + 4a^4 \ln a} \left[-\frac{1}{15} + \frac{49}{72}a^2 - \frac{2}{3}a^3 - \frac{1}{2}a^4 + \frac{38}{45}a^5 - \frac{7}{24}a^6 + \left(a^4 - \frac{4}{3}a^5 + \frac{1}{2}a^6\right) \ln a \right]$$

The expression for T_b obtained above is now substituted back into Eq. C5 to give the final expression for α_f, which is:

$$\alpha_f = \frac{2\lambda_L}{R_f - R_s} \left[1 - \left(\frac{R_s}{R_f - R_s}\right)^2 G(a) \right]^{-1} \quad \text{(C9)}$$

It may be rewritten in dimensionless form as:

$$Nu_f \equiv \frac{\alpha_f (R_f - R_s)}{\lambda_L} = 2 \left[1 - \left(\frac{R_s}{R_f - R_s}\right)^2 G(a) \right]^{-1} \quad \text{(C10)}$$

Equation C9 has been used simultaneously with Churchill and Bernstein's correlation for evaluating the fraction of the thermal resistance in the film in the total resistance against the gas-to-liquid heat transfer. The fraction has been found to be 0.1 to 0.2 under such operational conditions as to give flow pattern B. In practice this fraction should be even smaller due to the disturbances caused by falling drops. Thus, the use of assumption 8 listed in the "analysis of heat transfer" section is considered to be reasonable in view of the approximate nature of the analysis.

Manuscript received Apr. 29, 1993, and revision received Dec. 28, 1993.